$C(CH_3)_3$, 999-78-0; PhC≡CPh, 501-65-5; PhC≡CCH_3, 673-32-5; $H_3CCH(OH)C{\equiv}CCH(OH)CH_3$, 3031-66-1; $H_3CO_2CC{\equiv}CCO_2CH_3$, 762-42-5; $H_3CCO(CH_2)_4CH_3$, 110-43-0; $EtCOCH_2CH_3$, 96-22-0; $EtCH_2COCH_3$, 107-87-9; *n*-$PrCOCH_2CH_3$, 589-38-8; *n*-$PrCH_2COCH_3$, 591-78-6; *n*-$PrCOCH_2Pr$, 589-63-9; *t*-$BuCOCH_2CH_3$, 564-04-5; *t*-$BuCH_2COCH_3$, 590-50-1; $PhCOCH_2Ph$, 451-40-1; $PhCOCH_2CH_3$, 93-55-0; $PhCH_2COCH_3$, 103-79-7; H_3C-CH=CHCOCH(OH)CH_3, 127229-40-7; HC≡$C(CH_2)_4CH_3$, 628-71-7; 2,5-dimethyldihydro-3(2*H*)-furanone, 64026-45-5; Zeise's dimer, 12073-36-8.

Articles

Defluorination of Perfluoroolefins by Divalent Lanthanoid Reagents: Activating C–F Bonds

Patricia L. Watson,* Thomas H. Tulip, and Ian Williams

Central Research and Development Department,† E. I. du Pont de Nemours and Co., Experimental Station E328/333, P.O. Box 80328, Wilmington, Delaware 19880-0328

Received April 10, 1989

Divalent lanthanoid complexes $MCp^*_2{\cdot}L$ (M = Yb, Eu, Sm; L = diethyl ether or THF; Cp* = η^5-pentamethylcyclopentadienyl) and $YbCp'_2{\cdot}L$ (Cp' = η^5-methylcyclopentadienyl; L = tetrahydrofuran) rapidly abstract fluorine atoms from a variety of perfluoroolefins including perfluoro-2,4-dimethyl-3-ethylpent-2-ene, perfluoro-2,3-dimethylpent-2-ene, and perfluorocyclohexene. A similar abstraction of fluorine atoms from perfluorobenzene is much slower. However, visible light enhances the rate of fluorine abstraction from perfluorobenzene by $MCp^*_2{\cdot}OEt_2$ (M = Yb, Eu, Sm). Qualitative observation shows that the relative fluorine abstraction reactivity of the four lanthanoid complexes increases with increasingly negative reduction potential for reasonably unhindered fluoroolefin substrates. The Yb(III)/Yb(II) reduction potential of $YbCp'_2$ solvated in acetonitrile is determined here to be −1.65 V (relative to ferrocene) by cyclic voltammetry. The fully characterized organometallic products from the fluorine atom abstraction reactions are solvated trivalent lanthanoid fluorides $MCp^*_2F{\cdot}L$ (M = Yb, Eu, Sm; L = diethyl ether or THF) and $YbCp'_2F{\cdot}THF$. The molecular structures of $YbCp^*_2F{\cdot}OEt_2$ and $YbCp^*_2F{\cdot}THF$ determined by X-ray crystallography reveal the first terminal lanthanoid–fluoride bonds. However, three different environments for bridging lanthanoid–fluoride bonds are seen in the X-ray determined structure of the trivalent pentaytterbium cluster $[Yb_5Cp^*_6(\mu_4\text{-}F)(\mu_3\text{-}F)_2(\mu\text{-}F)_6]$, which is a secondary product from the further reaction of $YbCp^*_2F$ with perfluoroolefins. From the X-ray data of these three trivalent ytterbium compounds the *averaged* Yb–F distances are 2.02 Å for the terminal Yb–F bonding mode, 2.20 Å for an F atom bridging between two Yb atoms, and 2.37 Å for an F atom bridging between three of four Yb atoms.

Introduction

Homolytic bond energies of carbon–fluorine bonds are substantially higher than for analogous hydrocarbons. For example, the homolytic bond dissociation energy for $CF_4 \rightarrow CF_3 + F$ is 130.5 ± 3 kcal/mol,[1,2] whereas for $CH_4 \rightarrow CH_3 + H$ the energy is substantially less, 105 ± 1 kcal/mol.[2,3] The bond dissociation energy for $C_6F_6 \rightarrow C_6F_5 + F$ is even higher, 154.6 kcal/mol,[1] and the allylic bond dissociation energy for $CF_2CFCF_3 \rightarrow CF_2CFCF_2 + F$ is estimated to be around 120–126 kcal/mol.[4] However, since lanthanoid–fluorine bonds are also very strong (124–135 kcal/mol for trivalent Eu, Yb, and Sm[5]), the possibility of productive defluorination of fluorocarbons under mild conditions seems feasible. Indeed, in lanthanoid chemistry, Deacon[6] demonstrated selective intramolecular removal of fluorine from the ortho position of pentafluorobenzoic acid coordinated to ytterbium(II) during a complex protonolysis reaction. On the other hand, simple alkyl fluorides were shown by Finke et al. to be unreactive with divalent lanthanoid complexes[7] under mild conditions. Andersen[8] recently published a report of the fluorine atom abstraction reactions of the unsolvated divalent lanthanoid $YbCp^*_2$ with perfluorobenzene. Our

* To whom correspondence should be addressed.
† Contribution No. 4690.

(1) Smart, B. E. *Mol. Struct. Energ.* **1986**, *3*, 141–191.
(2) McMillen, D. F.; Golden, D. M. *Annu. Rev. Phys. Chem.* **1982**, *33*, 493–532.
(3) (a) Benson, S. W. *J. Chem. Educ.* **1965**, *42*, 502–518. (b) Castelhano, A. L.; Marriott, P. R.; Griller, D. J. *J. Am. Chem. Soc.* **1981**, *103*, 4262–4263.
(4) (a) The allylic CF_2CFCF_2–F bond dissociation energy (BDE) was roughly estimated (by B. E. Smart, Du Pont Central Research and Development Department) as BDE(CF_2CFCF_2–F) ~ BDE(CF_3CF_2–F), 126.8 kcal/mol[4c] − ΔG_{rot} (CF_2CFCF_2), 6.1 kcal/mol,[4d] = 120.7 kcal/mol. The corresponding hydrocarbon equation requires a correction factor of 2.4 kcal/mol, i.e. BDE(CH_2CHCH_2–H), 86.8 kcal/mol,[4e] = BDE(CH_3CH_2–H),[4e] 100.1 kcal/mol − ΔG_{rot}(CH_2CHCH_2), 15.7 kcal/mol,[4f] + 2.4 kcal/mol; the fluorocarbon reaction if corrected by the same amount gives BDE(CF_2CFCF_2–F) = 123.1 kcal/mol. (b) An alternative method gives a similar result. With an estimate in the JANAF tables[4g] for the heat of formation of CF_2CFCF_2, −159 kcal/mol, and the heats of formation of CF_2CFCF_3, −266.4 kcal/mol,[4h,i] and F, 18.9 kcal/mol, BDE(CF_2CFCF_2–F) = 125.9 kcal/mol. (c) McMillen, D. F.; Golden, D. M. *Annu. Rev. Phys. Chem.* **1982**, *33*, 493–532. (d) Smart, B. E.; Krusic, P. J.; Meakin, P.; Bingham, R. C. *J. Am. Chem. Soc.* **1974**, *96*, 7382–7383. (e) Griller, D.; Kanabus-Kaminska, J. M.; Maccoll, A. *J. Mol. Struct.* **1988**, *163*, 125–131. (f) Forth, H. G.; Trill, H.; Sustmann, H. *J. Am. Chem. Soc.* **1981**, *103*, 4483–4489. (g) *JANAF Thermochemical Tables*; Stull, D. R., Ed.; Dow Chemical: Midland, MI, 1965. (h) Duus, H. C. *Ind. Eng. Chem.* **1955**, *47*, 1445. (i) Dixon, D. A.; Fukunaga, T.; Smart, B. E. *J. Am. Chem. Soc.* **1986**, *108*, 4027–4031.

0276-7333/90/2309-1999$02.50/0

study focuses on the feasibility of this type of intermolecular fluorine abstraction using readily prepared divalent lanthanoids and includes the identification of both lanthanoid products and fluoroorganics from such reactions.

Typical conditions for defluorination of perfluorocycloalkanes currently involve the use of high temperature (600 °C) with graphitic carbon as a stoichiometric fluorine acceptor.[9] Rieke's activated magnesium also has been used to effect abstraction and substitution of a fluorine atom in hexafluorobenzene (albeit in very low yield).[10] Iron metal at 540 °C and platinum metal at 530–700 °C were successfully used to defluorinate perfluoroolefins, although cyclization of the resultant dienes as well as fragmentation reactions occurred readily at these temperatures.[11] Iron and nickel at 600 °C have defluorinated perfluoroethylbenzene to octafluorostyrene.[12] When zerovalent bis(arene)chromium complexes were used as radical initiators for hexafluoropropene oligomerization, the trimerization products identified were not simple olefins but rather were dienes.[13] Contrary to the mechanism proposed, these products were more likely the result of fluorine atom abstraction from the initially formed olefins by low-valent chromium. The last example implies that soluble low-valent transition-metal complexes may well provide low-temperature routes to defluorination of fluoroorganic materials. A recent report of fluorine abstraction in a tungsten complex provides another example, although this reaction was facilitated by being intramolecular.[14]

We report here the characterization of trivalent lanthanoid–fluoride complexes resulting from intermolecular abstraction of fluorine from perfluoroolefins by divalent lanthanoids. The driving forces for such reaction are the negative reduction potentials of the metal ions (in this case for the M(III)/M(II) couple), augmented by the formation of a very strong lanthanoid–fluoride bond. Finke et al. previously studied halogen abstraction reactions of R–I, R–Br, and R–Cl and showed these to be extremely fast inner-sphere atom abstraction processes.[7,15] We show that perfluoroolefins can be remarkably active, sometimes with reaction rates too fast to measure by conventional visible spectroscopy. The complexes $YbCp^*_2{\cdot}OEt_2$, $SmCp^*_2{\cdot}OEt_2$, $EuCp^*_2{\cdot}OEt_2$, and $YbCp'_2{\cdot}THF$ (note $Cp^* = \eta^5$-2-pentamethylcyclopentadienyl and $Cp' = \eta^5$-methylcyclopentadienyl) provide variation in reactivity resulting from differences in reduction potential and size of the coordination sphere.

Experimental Section

General Data. Unless otherwise stated all manipulations were carried out in a Vacuum Atmospheres nitrogen-purged glovebox or on a conventional glass high-vacuum line. Solvents were dried over and distilled from Na/benzophenone under prepurified nitrogen. C_5Me_5H (Cp*H, from Strem Chemical) was converted to KCp* by using KH in tetrahydrofuran (THF) at 25 °C. Elemental analyses were performed by Pascher Analytisches Laboratorium, Remagen, West Germany.

Preparations of crystalline THF-solvated divalent lanthanoid halides[16-23] are reported here together with characterization by elemental analysis, since different methods of isolation can yield products with varying degrees of solvation. For example, we obtained analyses for $YbI_2{\cdot}THF_{3-4}$ when this salt was isolated by merely evaporating a solution to dryness, whereas isolation by crystallization gave $YbI_2{\cdot}THF_2$. Previous reports of these compounds in the literature did not prove explicit stoichiometry. Isolation of crystalline materials as described here gives reliable stoichiometry for each of the salts.

Synthetic Procedures. MCp^*_2 (M = Yb, Sm, Eu) and $YbCp'_2$ as various solvates have been reported previously in the literature. References to those complexes are given below with our synthetic procedures for the diethyl ether solvates. Samples of C_9F_{18}, perfluoro-2,4-dimethyl-3-ethylpent-2-ene,[24] and C_7F_{14}, perfluoro-2,3-dimethylpent-2-ene,[25] were kindly provided by Dr. William Farnham of Du Pont Central Research and Development Department.

$YbBr_2{\cdot}THF_2$. Yb metal (40 mesh, Cerac, 25 g, 0.143 mol, excess) was slurried in THF (400 mL). Dibromoethane (21.5 g, 0.114 mol, dried with activated molecular sieves) in THF (50 mL) was added slowly to the slurry over 1 h. Ethylene bubbled from the reaction mixture, which was then stirred for 3 days in a flask covered with foil to eliminate light. THF (500 mL) was added to the mixture, which was gently swirled allowing the heavy unreacted metal to sink to the bottom. The slurry of suspended light olive-green THF-solvated $YbBr_2$ was decanted from the top into a medium-porosity frit for filtration. The filtrate was recycled as necessary to dilute the slurry and aid separation of the solids. The light green solids isolated by this filtration were dried under vacuum overnight. Yield: 43 g, 79%. Anal. Calcd for $C_8H_{16}Br_2O_2Yb$: C, 20.14; H, 3.38; O, 6.71; Br, 33.50; Yb, 36.27. Found: C, 19.6; H, 3.33; O, 6.8; Br, 33.1; Yb, 36.5.

$YbI_2{\cdot}THF_2$. Yb metal (40 mesh, Cerac, 10 g, 0.057 mol, excess) was slurried in THF (400 mL). Diiodoethane (13.44 g, 0.048 mol), freshly recrystallized from ether, was added to the slurry. Ethylene bubbled from the reaction mixture, and the temperature rose from 27 to 58 °C during the first hour of the reaction. The mixture was stirred overnight in a flask covered with foil to eliminate light. THF (500 mL) was added to the mixture, which was then gently heated until all the solids were in solution and filtered to remove any extraneous metal. The pale yellow filtrate was evaporated to about 150-mL volume under vacuum and then was cooled to

(5) Huheey, J. E. *Inorganic Chemistry: Principles of Structure and Reactivity*, 2nd ed.; Harper and Row: New York, 1978; p 845. Data therein was obtained from: Feber, R. C. Los Alamos Report LA-3164, 1965.

(6) (a) Deacon, G. B.; MacKinnon, P. I. *Tetrahedron Lett.* **1984**, *25*, 783–784. (b) Deacon, G. B.; MacKinnon, P. I.; Tuong, T. D. *Aust. J. Chem.* **1983**, *36*, 43–53.

(7) Finke, R. G.; Keenan, S. R.; Schiraldi, D. A.; Watson, P. L. *Organometallics* **1987**, *6*, 1356–1358.

(8) Burns, C. J.; Andersen, R. A. *J. Chem. Soc., Chem. Commun.* **1989**, 136–7.

(9) Patrick, C. R.; Pedler, A. E.; Seabra, A.; Stephens, R.; Tatlow, J. C. *Chem. Ind. (London)* **1963**, 1557–1558.

(10) (a) Rieke, R. D.; Bales, S. E. *J. Chem. Soc., Chem. Commun.* **1973**, 879–880. (b) Rieke, R. D.; Hundnall, P. M. *J. Am. Chem. Soc.* **1972**, *94*, 7178–7179.

(11) (a) Chambers, R. D.; Lindley, A. A.; Fielding, H. C.; Moilliet, J. S.; Whittaker, G. *J. Chem. Soc., Perkin Trans. 1* **1981**, 1064–1067. (b) Chambers, R. D.; Lindley, A. *J. Chem. Soc., Chem. Commun.* **1978**, 475–476.

(12) Letchford, B. R.; Patrick, C. R.; Stacey, M.; Tatlow, J. C. *Chem. Ind. (London)* **1962**, 1472–1473.

(13) Huang, Y.; Li, J.; Zhou, J.; Wang, Q.; Gui, M. *J. Organomet. Chem.* **1981**, *218*, 169–175. Our results suggest an alternative mechanism for formation of C_9F_{16} dienes, which does not require the intermediate formation of C_9HF_{17} invoked in this paper.

(14) Richmond, T. G.; Osterberg, C. E.; Arif, A. M. *J. Am. Chem. Soc.* **1987**, *109*, 8091–8092.

(15) Finke, R. G.; Keenan, S. R.; Schiraldi, D. A.; Watson, P. L. *Organometallics* **1986**, *5*, 598–601.

(16) Eick, H. A. *J. Less Common Met.* **1987**, *127*, 7–17.

(17) Watson, P. L. *J. Chem. Soc., Chem. Commun.* **1980**, 652–653.

(18) Evans, W. J.; Grate, J. W.; Choi, H. W.; Bloom, I.; Hunter, W. E.; Atwood, J. L. *J. Am. Chem. Soc.* **1985**, *107*, 941–946.

(19) Howell, J. K.; Pytlewski, L. L. *J. Less Common Met.* **1969**, *18*, 437–439.

(20) Suleimanov, G. Z.; Bregadze, V. I.; Koval'chuk, N. A.; Khalilov, Kh. S.; Beletskaya, I. P. *J. Organomet. Chem.* **1983**, *255*, C5–C7.

(21) Imamoto, T.; Ono, M. *Chem. Lett.* **1987**, 501–502.

(22) Namy, J. L.; Girard, P.; Kagan, H. B. *Nouv. J. Chim.* **1977**, *1*, 5–7.

(23) Girard, P.; Namy, J. L.; Kagan, H. B. *J. Am. Chem. Soc.* **1980**, *102*, 2693–2698.

(24) (a) Scherer, K. V.; Ono, T.; Yamanouch, K.; Fernandez, R.; Henderson, P. *J. Am. Chem. Soc.* **1985**, *107*, 718–719. (b) Dmowski, W.; Flowers, W. T.; Haszeldine, R. N. *J. Fluorine Chem.* **1977**, *9*, 94–96. (c) Ishikawa, N.; Sekiya, A. *Nippon Kagaku Kaishi* **1972**, 2214–2215. (d) Ishikawa, N.; Maruta, M. *Nippon Kagaku Kaishi* **1977**, 1411–1415.

(25) Fields, R.; Haszeldine, R. N.; Kumadaki, I. *J. Chem. Soc., Perkin Trans. 1* **1982**, 2211–2217.

−30 °C until crystals formed. The pale yellow-green crystalline product was collected by filtration, washed with cold ether, and dried under vacuum for 1 h at room temperature. The filtrate was again concentrated in this manner to obtain a second crop. Total yield: 24.1 g, 88%. Anal. Calcd for $C_8H_{16}I_2O_2Yb$: C, 16.83; H, 2.82; I, 44.44; Yb, 30.30. Found: C, 16.08; H, 2.71; I, 45.3; Yb, 30.3.

EuI_2·THF_2. Eu metal (40 mesh, Cerac, 19.6 g, 0.129 mol, excess) was slurried in THF (400 mL). Diiodoethane (29.06 g, 0.103 mol), freshly recrystallized from ether, was added to the slurry. Ethylene bubbled from the reaction mixture, and the temperature rose from 27 to 54 °C during the first hour of the reaction. The purplish mixture was then stirred overnight in a foil-covered flask. THF (500 mL) was added to the mixture, which was gently heated until all the solids were in solution, and then was filtered to remove any extraneous metal. The somewhat fluorescent-looking light green filtrate was evaporated to about 150-mL volume under vacuum and then cooled to −30 °C until crystals formed. The pale yellow-green crystalline product was collected by filtration, washed with cold ether, and dried under vacuum for 1 h at room temperature (41.7 g). The filtrate was again concentrated in this manner to obtain a second crop. Total yield: 9.8 g, 72%. Anal. Calcd for $C_8H_{16}EuI_2O_2$: C, 17.47; H, 2.93; I, 46.15; Eu, 27.63. Found: C, 17.53; H, 2.94; I, 46.3; Eu, 28.2.

SmI_2·THF_2. Sm metal (40 mesh, Cerac, 20 g, 0.133 mol, excess) was slurried in THF (400 mL). Diiodoethane (30 g, 0.106 mol), freshly recrystallized from ether, was added to the slurry. Ethylene bubbled from the reaction mixture, and the temperature rose from 27 to 61 °C during the first hour of the reaction. The dark green-blue mixture was then stirred overnight in a foil-covered flask. THF (500 mL) was added to the mixture, which was then gently heated until the solids dissolved, and then filtered. The filtrate was evaporated to about 400-mL volume under vacuum and then cooled to −30 °C until crystals formed. The dark blue crystalline product was collected by filtration, washed with cold ether, and dried under vacuum for 1 h at room temperature (44.3 g). The filtrate was again concentrated to 100 mL to obtain a second crop. Total yield: 70%, 10 g. Anal. Calcd for $C_8H_{16}I_2O_2Sm$: C, 17.52; H, 2.94; I, 46.28; Sm, 27.42. Found: C, 17.35; H, 2.93; I, 46.8; Sm, 27.6.

YbCp*$_2$·OEt_2.[17] KCp* (3.8 g, 0.022 mol) was added in two equal portions to a stirred solution of $YbBr_2$·THF_2 (4.7 g, 0.01 mol) in THF (100 mL). Addition of half the KCp* yielded an orange-red solution of THF-solvated YbBrCp*, which turned red-purple on addition of the remainder of KCp*. The mixture was stirred for 30 min at 25 °C and then filtered through a medium-porosity frit to remove any extraneous debris. The filtrate was stripped to dryness under vacuum. Rigorously dried ether (150 mL) was added to the red filtrate residues, and the resulting brown solution was stirred over low heat under a slow flow of prepurified nitrogen until dry. Ether (150 mL) was added to the dry solids giving a green solution, which was again reduced to dryness under nitrogen with gentle heat. Residues were taken up in either (150 mL), and the solution was filtered through a medium-porosity frit. The resulting filtrate was cooled to −25 °C and then was filtered, yielding green crystals (1.84 g). The filtrate was reduced in volume to 50 mL, cooled to −25 °C, and filtered, yielding a second crop of green crystals (2.36 g). Total yield: 4.2 g, 81%. The compound is prepared from YbI_2THF_2 in an analogous fashion to that for $YbBr_2THF_2$. Anal. Calcd for $C_{24}H_{40}OYb$: C, 55.69; H, 7.79; Yb, 33.43. Found: C, 55.75; H, 8.03; Yb, 33.31. ^{1}H NMR (benzene-d_6): 0.878 (CH_3, ether), 2.125 (CH_3, Cp*), 2.95 (CH_2, ether) ppm; the ratio of C_5Me_5 to ether was 2:1.

EuCp*$_2$·OEt_2.[26] KCp* (8.0 g, 0.45 mol) was added to a stirred pale yellow-green solution of EuI_2·THF_2 (11.0 g, 0.02 mol) in THF (200 mL). The orange mixture of EuCp*$_2$·THF_n was stirred for 2 h at 25 °C and then filtered through a medium-porosity frit to remove KI. The filtrate was stripped to dryness under vacuum. Rigorously dried ether (150 mL) was added to the filtrate residues, and the resulting brown-orange solution was stirred over low heat under a slow flow of prepurified nitrogen until dry. Twice again, ether (150 mL) was added to the dry solids and the solution was reduced to dryness under nitrogen with gentle heat. Residues were then taken up in ether (150 mL), and the solution was filtered through a medium-porosity frit to remove any extraneous debris. The filtrate was cooled to −25 °C to yield a first crop of dark orange-tan crystals (5.5 g, 50%), isolated by decanting the supernatant liquid and drying the crystals under vacuum. Anal. Calcd for $C_{24}H_{40}EuO$: C, 58.08; H, 8.12; Eu, 30.60. Found: C, 57.79; H, 8.06; Eu, 30.5. ^{1}H NMR (benzene-d_6/H$^+$) showed ratio of C_5Me_5H to ether was 2:1.

SmCp*$_2$·OEt_2.[27] KCp* (7.8 g, 0.045 mol) was added to a stirred solution of dark blue SmI_2·THF_2 (10.2 g, 0.0186 mol) in THF (200 mL). The mixture was stirred for 2 h at 25 °C and then was filtered through a medium-porosity frit. The filtrate was stripped to dryness under vacuum. Rigorously dried ether (150 mL) was added to the red-brown filtrate residues and the resulting solution was stirred over low heat under a slow flow of prepurified nitrogen until dry. Twice again, ether (150 mL) was added to the dry solids and the solution was reduced to dryness under nitrogen with gentle heat. Residues were then taken up in ether (150 mL), and the green-brown solution was filtered through a medium-porosity frit. The filtrate was cooled to −25 °C to yield a first crop of black crystals (5.4 g, 56%), isolated by decanting the supernatant liquid and drying the crystals under vacuum. Anal. Calcd for $C_{24}H_{40}OSm$: C, 58.24; H, 8.15; Sm, 30.38. Found: C, 58.36; H, 8.06; Sm, 30.4. ^{1}H NMR (benzene-d_6/H$^+$) showed ratio of C_5Me_5H to ether was 2:1.

Yb(C_5H_4Me)$_2$ and Yb(C_5H_4Me)$_2$THF.[28,29] KC_5H_4Me (4.95 g, 0.042 mol) was added to a slurry of $YbBr_2$·THF_2 (10 g, 0.021 mol) in THF (100 mL). The solution turned the deep purple color of Yb(C_5H_4Me)$_2$·THF_n. After being stirred for 3 h, the solution was filtered and the purple filtrate was evaporated to dryness, giving yellow solids of Yb(C_5H_4Me)$_2$·THF_2: 9.2 g, 92%. This material was slurried in ether and then was filtered off (50 mL each wash) several times until the supernatant ether wash was colorless. The solids then were dried under vacuum, giving greenish yellow Yb(C_5H_4Me)$_2$. Anal. Calcd for $C_{12}H_{14}Yb$: C, 43.51; H, 4.26; Yb, 52.23. Found: C, 43.61; H, 4.3; Yb, 51.9. ^{1}H NMR (glyme-d_{10}): 5.55, 5.49, 2.10 ppm (2:2:3); no ether or THF in spectrum. Since Yb(C_5H_4Me)$_2$ is insoluble in ether, 1 equiv of THF was added to a slurry of Yb(C_5H_4Me)$_2$ in ether and the mixture was evaporated to dryness, giving yellow-gold Yb(C_5H_4Me)$_2$THF (stoichiometry confirmed by NMR) which is slightly more soluble in ether.

YbCp*$_2$F·OEt_2. Solutions of YbCp*$_2$·OEt_2 (0.398 g, 0.00077 mol) in ether (15 mL) and C_7F_{14}, perfluoro-2,3-dimethylpent-2-ene (0.135 g, 0.00039 mol), in ether (5 mL) were cooled to −25 °C. The fluorocarbon solution was then added to the stirred green YbCp*$_2$·OEt_2 solution. The mixture was allowed to warm to 25 °C over 30 min (during which the color changed to a deep orange) and then evaporated to dryness. Residues were taken up in ether (2 mL) and cooled at −25 °C until crystals formed (about 2 days). The red-orange crystals were separated by decanting the supernatant and drying the residual solids under vacuum. A second crop of crystals was obtained from the supernatant in the same manner. Anal. Calcd. for $C_{24}H_{40}FOYb$: C, 53.72; H, 7.51; F, 3.54; Yb, 32.25. Found: C, 53.70; H, 7.31; F, 2.85; Yb, 32.3. ^{1}H NMR (benzene-d_6/H$^+$) showed ratio of C_5Me_5H to ether was 2:1. IR (Nujol mull between polyethylene film): ν(Yb–F) 303 cm^{-1}.

YbCp*$_2$F·THF. A solution of YbCp*$_2$F·OEt_2 was dissolved in THF. The mixture was then evaporated to dryness, quantitatively giving YbCp*$_2$F·THF as an orange-red powder. The complex was recrystallized from toluene by cooling a saturated solution to −25 °C for several days. ^{1}H NMR (benzene-d_6/H$^+$) showed the ratio of C_5Me_5H to THF was 2:1.

EuCp*$_2$F·OEt_2. Solutions of EuCp*$_2$·OEt_2 (0.398 g, 0.0077 mol) in ether (15 mL) and C_7F_{14}, perfluoro-2,3-dimethylpent-2-ene (0.135 g, 0.0039 mol), in ether (5 mL) were cooled to −25 °C. The

(26) Andersen, R. A.; Boncella, J. M.; Burns, C. J.; Green, J. C.; Hohl, D.; Roesch, N. *J. Chem. Soc., Chem. Commun.* **1986**, 405–407.

(27) Evans, W. J.; Hughes, L. A.; Hanusa, T. P. *J. Am. Chem. Soc.* **1984**, *106*, 4270–4272.

(28) Deacon, G. B.; MacKinnon, P. I.; Hambley, T. W.; Taylor, J. C. *J. Organomet. Chem.* **1983**, *259*, 91–97.

(29) (a) Deacon, G. B.; Newnham, R. H. *Aust. J. Chem.* **1985**, *38*, 1757–65. (b) Zinnen, H. A.; Pluth, J. J.; Evans, W. J. *J. Chem. Soc., Chem. Commun.* **1980**, 810–812.

fluorocarbon solution was then added to the stirred brown $EuCp^*_2{\cdot}OEt_2$ solution. The mixture was allowed to warm to 25 °C over 30 min (during which the color changed to a deep orange) and then was evaporated to dryness. Residues were taken up in ether (2 mL) and cooled at −25 °C until crystals formed (about 2 days). The orange-red crystals were separated by decanting the supernatant and drying the residual solids under vacuum. A second crop of crystals was obtained from the supernatant. Anal. Calcd for $C_{24}H_{40}FOEu$: C, 55.91; H, 7.82; Eu, 29.48. Found: C, 56.2; H, 7.9; Eu, 29.32. ^1H NMR (benzene-d_6/H^+) showed the ratio of C_5Me_5H to ether was 2:1. IR (Nujol mull between polyethylene film): ν(Eu–F) 311 cm^{-1}.

$SmCp^*_2F{\cdot}OEt_2$. Solutions of $SmCp^*_2{\cdot}OEt_2$ (0.396 g, 0.0008 mol) in ether (30 mL) and C_7F_{14}, perfluoro-2,3-dimethylpent-2-ene (0.135 g, 0.0004 mol), in ether (10 mL) were cooled to −25 °C. The fluorocarbon solution was then added to the stirred green-black $SmCp^*_2{\cdot}OEt_2$ solution. The mixture was allowed to warm to 25 °C over 30 min (after an immediate color change to yellow) and was then evaporated to dryness. Residues were taken up in ether (5 mL) and cooled at −25 °C until crystals formed (about 1 week). The yellow crystals were separated by decanting the supernatant and drying the residual solids under vacuum. Two further crops were obtained from the supernatant. Anal. Calcd for $C_{24}H_{40}FOSm$: C, 56.09; H, 7.85; Sm, 29.25. Found: C, 55.69; H, 7.49; Sm, 30.1. ^1H NMR (benzene-d_6/H^+) showed the ratio of C_5Me_5H to ether was 2:1. IR (Nujol mull between polyethylene film): ν(Sm–F) 304 cm^{-1}.

$Yb(C_5H_4Me)_2F{\cdot}THF$. Solutions of $Yb(C_5H_4Me)_2$ (0.405 g, 0.00122 mol) in THF (10 mL) and C_7F_{14}, perfluoro-2,3-dimethylpent-2-ene (0.213 g, 0.0006 mol), in THF (5 mL) were cooled to −25 °C. The fluorocarbon solution was then added to the stirred purple $Yb(C_5H_4Me)_2{\cdot}THF_2$ solution. The mixture was allowed to warm to 25 °C over 30 min (during which the color changed to orange) and was then evaporated to dryness. Residues were taken up in ether/THF (2 mL/2 mL) and cooled at −25 °C until crystals formed (about 1 day). The orange crystals were separated by decanting the supernatant and drying the residual solids under vaccum. Anal. Calcd for $C_{16}H_{22}FOYb$: C, 45.50; H, 5.25; Yb, 40.97. Found: C, 45.33; H, 5.19; Yb, 40.7. ^1H NMR (benzene-d_6/H^+) showed the ratio of C_5H_5Me to ether was 2:0.97. IR (Nujol mull between polyethylene film): ν(Yb–F) 326 cm^{-1}.

$[Yb_5Cp^*_6(\mu_4\text{-}F)(\mu_3\text{-}F)_2(\mu\text{-}F)_6]$, Toluene Solvate. Approximately 1 equiv of C_9F_{18}, perfluoro-2,4-dimethyl-3-ethylpent-2-ene, was added to a green solution of $YbCp^*_2{\cdot}OEt_2$ (0.5 g) in toluene (5 mL). The resulting orange solution was left for 9 weeks at ambient temperature. Small red crystals (about 80 mg) precipitated and were collected for X-ray crystallographic studies. [This procedure was followed twice, but no attempt was made to optimize the reaction.]

Cyclic Voltammetry. Cyclic voltammetric experiments with $YbCp'_2$ (0.002 M, which gives a green solution in acetonitrile) were conducted at a polished platinum electrode in a solution of 0.1 M NBu_4PF_6 in acetonitrile using a Princeton Applied Research Model 173 potentiostat and Model 175 universal programmer at scan rates, ν, of 20–200 mV/s. A platinum counter electrode and a silver chloride-coated silver wire reference electrode were used. A reversible Yb(III)/Yb(II) couple due to $YbCp'_2(acetonitrile)_n^{1+/0}$ was observed 1.65 V more cathodic than ferrocene, which was added subsequently as an internal reference[30] (both couples showed anodic peak potential to cathodic peak potential separations of about 100 mV). Exactly the same conditions just described were used to obtain the M(III)/M(II) reduction potentials of $MCp^*_2(acetonitrile_n$, M = Eu, Yb, and Sm (formed in situ from $MCp^*_2{\cdot}$ether in acetonitrile solution): $EuCp^*_2$, −1.22 V; $YbCp^*_2$, −1.78 V; $SmCp^*_2$, −2.41 V relative to ferrocene. It should be noted that the solvent acetonitrile must be extremely pure and dry in order to observe good reversible cyclic voltammograms. The acetonitrile used here was distilled from calcium hydride and then was dried over 3-Å molecular sieves three times prior to use. Before use, the solution of NBu_4PF_6 in acetonitrile was passed through a 2-in. column of activated alumina. The platinum electrode was repolished between each measurement.

In all cases the anodic peak potential to cathodic peak potential separations were greater than 59 mV (usually 80–100 mV), but the separations were the same as for the ferrocene peak when ferrocene was added to the solution as internal reference. This observation was therefore attributed to internal resistance in the electrochemical cell rather than lack of electrochemical reversibility. With freshly cleaned and polished electrodes, the anodic peak current and cathodic peak currents in each case were equal at scan rates, υ, of greater than 100 mV/s. For $YbCp^*_2(acetonitrile)_n$, a plot of $\upsilon^{1/2}$ versus peak current was linear for values of υ = 20, 50, 100, and 200 mV/s, clearly demonstrating electrochemical reversibility.

Visible Absorption Spectra. Divalent starting materials MCp^*(or Cp′)$_2{\cdot}$solvent and isolated trivalent product MCp^*(or Cp′)$_2$F·solvent compounds all showed visible spectra with uncomplicated Beer's law behavior over the concentration range 3×10^{-4} to 1×10^{-2} M. Spectra were recorded by using a Perkin-Elmer 330 spectrophotometer with samples contained in airtight 1-cm quartz cells. Absorption maxima (and extinction coefficients) are as follows: $YbCp^*_2{\cdot}OEt_2$ in ether, 680 (ϵ = 221), 465 (350), 405 nm (418); $EuCp^*_2{\cdot}OEt_2$ in ether, 570 (ϵ = 121, shoulder), 460 (349), 390 nm (434); $SmCp^*_2{\cdot}OEt_2$ in ether, 710 (ϵ = 143), 500 (134), 395 nm (390); $Yb(C_5H_4Me)_2$ in glyme, 635 (ϵ = 250), 385 nm (511); $YbCp^*_2F{\cdot}OEt_2$ in ether, 475 nm (ϵ = 230); $YbCp^*_2F{\cdot}OEt_2$ in glyme, 465 nm (ϵ = 222); $EuCp^*_2F{\cdot}OEt_2$ in ether, 580 nm (ϵ = 182); $SmCp^*_2F{\cdot}OEt_2$ in ether, 375 nm (ϵ = 448); $Yb(C_5H_4Me)_2F$ in glyme (tail of UV band, no distinct maximum, 370 nm chosen arbitrarily) 370 nm (ϵ = 173).

General Procedure for Fluorine Abstraction Reactions and Analysis. All reactions were carried out in a Vacuum Atmospheres nitrogen-purged drybox using oven-dried glassware. The reaction vessels used were sealable 10-mL glass tubes with Teflon stopcocks and vacuum line adapters. The lanthanoid reagent (usually 0.00005–0.0002 mol) was weighed and transferred to the vessel as a solid. Two 200-μL washes of the weighing vessel with the desired solvent or solvent mixture made the transfer quantitative. A small Teflon-covered stir bar was added. The fluorinated substrate (usually 0.25–1 equiv based on lanthanoid reagent) was weighed, or accurately syringed (having determined the density), and then added to 200 μL of the NMR reference solution (0.15 M trifluorotoluene in C_6D_6) plus 200 μL of the desired solvent (in control experiments trifluorotoluene was shown not to react with any reagent under the conditions of these experiments). The substrate solution was then added to the stirred lanthanoid solution (total volume 800 μL), and the stopcock was sealed. After the desired length of time at the desired temperature, the reaction vessel was transferred to the vacuum line and the volatiles were transferred under vacuum to an NMR tube that was then sealed off. The proton-decoupled 188-MHz ^{19}F NMR spectrum[31] and occasionally the 360-MHz ^1H NMR spectrum (Nicolet 360) were then observed. [A Nicolet 200 NMR spectrometer was used, with spectra referenced to CCl_3F = 0, using $CF_3C_6H_5$ as internal standard at 62.57 ppm to higher field of CCl_3F. All spectra reported have resonances given as positive parts per million values which are at higher field than CCl_3F and which may be assumed to be a singlet or unresolved multiplet unless otherwise stated.] Subsequently, selected samples were opened and examined by GC–MS[11,12,32] on a spectrometer with the capability to perform accurate mass measurements. [A VG-7070 HS mass spectrometer was used, with 2-m Porapak Q column at 150–220 °C (column A) or a 30-m DB-210 column at 30–240 °C (column B): 10°/min; flow 20 mL of He/min. Retention times are given in minutes.] Yields and total recoveries are based on ^{19}F NMR integration of products and starting material against the internal standard $CF_3C_6F_5$ of known concentration. Data obtained in this manner is listed for each of the fluorocarbons identified.

C_9F_{18}, perfluoro-2,4-dimethyl-3-ethylpent-2-ene:[24] ^{19}F NMR (diethyl ether 75%, benzene-d_6 25%, 25 °C) 56.1 (76%) and 56.5 (24%, total 3 F), 58.3 (76%) and 58.7 (24%, total 3F), 70 (v br,

(30) (a) $E_0[Fe(C_5H_5)_2^{0/1+}]$ = 0.315 V in acetonitrile at platinum electrode versus SCE: Little, W. F.; Reilley, C. N.; Johnson, J. D.; Lynn, K. N.; Sanders, A. P. *J. Am. Chem. Soc.* **1964**, *86*, 1376–1381. (b) Koepp, H. M.; Wendt, H.; Strehlow, H. *Z. Elektrochem.* **1960**, *64*, 483–491.

(31) For a compilation 19F NMR data and trends, see: Weigert, F. J.; Karel, K. J. *J. Fluorine Chem.* **1987**, *37*, 125–149.

(32) "*Mass Spectrometry of Fluorine Compounds*". Majer, J. R. *Adv. Fluorine Chem.* **1961**, *2*, 55–103.

6 F), 70.5 (3 F), 92 (br, 2 F), 155.4 (24%) and 156.8 ppm (76%; conformers, total 1 F); Temperature-dependent ^{19}F NMR (diethyl ether, −20 °C) 57.1 (60%) and 57.8 (40%, total 3 F), 59.3 (60%) and 59.7 (40%, total 3 F), 68 (3 F), 71.1 (3 F), 73.3 (3 F), 93.2 (2 F), 157.1 and 160.7 ppm (total 1 F); temperature-dependent ^{19}F NMR (diethyl ether, +40 °C) 57 and 57.7 (total 3 F), 59.25 and 59.6 (total 3 F), 70.6 (br, 6 F), 71.4 (3 F), 92.9 (br, 2 F), 156.5 and 160.1 ppm (total 1 F); GC–MS column A, rt = 11.0 min, column B, rt = 11.0 min, *m/e* for parent calcd 430.9728, found 430.9686 (rt = retention time).

C_9F_{16}, perfluoro-2-methyl-3-isopropylpenta-1,3-diene:[13] ^{19}F NMR (diethyl ether 75%, benzene-d_6 25%) 59.0 (3 F), 65.1 (1 F), 67.2 (1 F), 67.8 (3 F), 73.1 (3 F), 75.3 (3 F), 95.0 (1 F), 172.5 ppm (1 F); GC–MS column A, rt = 7.52 min, column B, rt = 8.83 min, *m/e* for parent calcd 411.9744, found 411.9734.

C_9F_{16}, perfluoro-2,4-dimethyl-3-ethylpenta-1,3-diene:[13] ^{19}F NMR (diethyl ether 75%, benzene-d_6 25%) 57.9 (3 F), 58.1 (3 F), 59.6 (3 F), 66.5 (1 F), 68.8 (1 F), 79.6 (3 F), 106.7 (1 F), 106.9 ppm (1 F); GC–MS column A, rt = 7.52 min, column B, rt = 8.83 min, not resolved from isomer.

C_9F_{14}, perfluoro-2,4-dimethyl-3-ethylidenepenta-1,4-diene: ^{19}F NMR (diethyl ether 75%, benzene-d_6 25%) 58.6 (3 F), 59.3 (3 F, dd, app J = 10, 17 Hz), 67.3 (1 F, br m), 68.3 (1 F), 68.7 (3 F, d, app J = 8 Hz), 69.7 (1 F), 103.6 ppm (1 F); GC–MS column A, rt = 7.2 min, column B, rt = 9.19 min, *m/e* for parent calcd 373.9776, found 373.9791.

C_7F_{14}, perfluoro-2,3-dimethylpent-2-ene:[11] ^{19}F NMR (diethyl ether 75%, benzene-d_6 25%) 57.3 (3 F), 58.2 (3 F), 58.7 (3 F), 73.8 (3 F), 98.6 ppm (2 F); GC–MS column A, rt = 4.32 min, *m/e* for parent − F calcd 330.9792, found 330.9786.

C_7F_{12}, perfluoro-2-methyl-3-ethylbuta-1,3-diene: ^{19}F NMR (diethyl ether 75%, benzene-d_6 25%) 59.35 (3 F), 64 (1 F, q), 64.2 (1 F), 66.2 (1 F), 67.9 (1 F), 84.9 (3 F), 112 ppm (2 F, dm); GC–MS column A, rt = 4.08 min, *m/e* for parent calcd 311.9808, found 311.9799.

C_7F_{12}, perfluoro-(*E*)-2,3-dimethylpenta-1,3-diene:[33] ^{19}F NMR (diethyl ether 75%, benzene-d_6 25%) 59.5 (3 F), 61.5 (3 F, d), 65.9 (1 F), 68.1 (1 F), 68.9 (3 F, s), 101.7 ppm (1 F); GC–MS column A, rt = 3.6 min, *m/e* for parent calcd 311.9808, found 311.9825.

C_7F_{12}, perfluoro-(*Z*)-2,3-dimethylpenta-1,3-diene:[33] ^{19}F NMR (diethyl ether 75%, benzene-d_6 25%) 57.6 (3 F), 59.1 (3 F), 67.1 (1 F, qd), 67.5 (3 F), 68.3 (1 F), 99.1 ppm (1 F); GC–MS column A, rt = 3.6 min, not resolved from *E* isomer.

C_6F_{10}, perfluorocyclohexene (PCR Chemical): ^{19}F NMR (diethyl ether 75%, benzene-d_6 25%) 118.0 (4 F, m), 132.8 (4 F, m), 150.4 ppm (2 F, m); GC–MS column A, rt = 3.2 min, *m/e* for parent calcd 261.984, found 261.9786.

C_6HF_9, 2,3,3,4,4,5,5,6,6-nonafluorocyclohexene:[34] ^{19}F NMR (diethyl ether 75%, benzene-d_6 25%) 106.1 (2 F), 120.2 (2 F), 122.3 (vinylic, 1 F), 133.8 (2 F), 134.3 ppm (2 F); GC–MS column A, rt = 4.72 min, *m/e* for parent − F calcd 224.995, found 224.9994.

$C_6H_2F_8$, 3,3,4,4,5,5,6,6-octafluorocyclohexene:[35] ^{19}F NMR (diethyl ether 75%, benzene-d_6 25%) 108.8 (4 F, m), 134.8 ppm (4 F, m); GC–MS column A, rt = 7.7 min, *m/e* for parent − F calcd 207.0044, found 207.0071.

C_6HF_5, pentafluorobenzene (PCR Chemical): ^{19}F NMR (diethyl ether 75%, benzene-d_6 25%) 138.8 (2 F, dd, J = 20, 8 Hz), 154.3 (1 F, *t*, J = 22 Hz), 162.5 (2 F, app t, J = 21 Hz, of d, J = 8 Hz); GC–MS column A, rt = 6.32 min, *m/e* for parent calcd 167.9998, found 167.9996.

C_6F_6, hexafluorobenzene (PCR Chemical): ^{19}F NMR (diethyl ether 75%, benzene-d_6 25%) 162.7 ppm; GC–MS column A, rt = 5.76 min, *m/e* for parent calcd 185.9904, found 185.9896.

$C_{12}F_{10}$, decafluorobiphenyl: ^{19}F NMR (diethyl ether 75%, benzene-d_6 25%) 138.0 (4 F, m), 150.0 (2 F, t, J = 21 Hz), 160.7 ppm (4 F, m). GC–MS column B, rt = 16.64 min, *m/e* for parent calcd 333.9976, found 333.9957.

Table I. Summary of Selected Crystal and Refinement Data

	$YbCp^*_2F\cdot OEt_2$	$YbCp^*_2F\cdot THF$	$[Yb_5Cp^*_6F_9]\cdot C_6H_5CH_3$
(a) Crystal Data			
formula	$C_{24}H_{40}FOYb$	$C_{24}H_{38}FOYb$	$C_{30}H_{90}F_9Yb_5\cdot C_7H_8$
fw	536.62	534.61	1939.72
color	dark red	dark red	dark red
size, mm	0.26 × 0.28 × 0.30	0.34 × 0.14 × 0.31	0.20 × 0.34 × 0.36
cryst system	orthorhombic	monoclinic	monoclinic
space group	*Pbca*, No. 61	$P2_1/c$, No. 14	$P2_1/n$, No. 14
(b) Unit-Cell Parameters (Mo Kα Radiation; λ = 0.71069 Å; −100 °C)			
a, Å	14.711 (2)	14.906 (2)	23.308 (4)
b, Å	15.865 (2)	9.108 (2)	14.645 (3)
c, Å	20.300 (3)	17.104 (2)	20.875 (3)
α, deg	90	90	90
β, deg	90	97.686 (1)	107.96 (1)
γ, deg	90	90	90
V, Å^3	4738	2301	6778
Z	8	4	4
D_{calcd}, g·cm^{-3}	1.505	1.54	1.901
(c) Data Collected on a Syntex P3 Diffractometer at −100 °C			
min, max 2θ	4, 55	4, 52	4.6, 48
μ(Mo), cm^{-1}	39.55	42.96	68.73
reflctns measd	6062	5093	11429
transmissn factors	0.22–0.33	0.60–1.0	0.09–0.18
(d) Full-Matrix Least-Squares Refinement			
reflctns refined	2865	4989	7322
$I = n(I)$, *n*	2	3	3
$R = \sum\|\|F_o\| - \|F_c\|\|/\sum\|F_o\|$	0.038	0.031	0.033
R_w	0.035	0.034	0.031
method	heavy-atom Patterson	heavy-atom Patterson	MULTAN
max resid density, e/Å^3	1.14	0.27–0.65	1.12
assoc with	C_2,C_4 of ether	Yb	toluene ring

Reactions Catalyzed by Light. Samples were prepared in a Pyrex tube exactly as described for the fluorine abstractions. The tube was placed in front of a high-intensity (200 ft-c at 1 ft) tungsten lamp on the maximum setting. The setup was also placed in fron of a fan for cooling, and the temperature was monitored to prevent heating of the sample. Several experiments were performed with light filtered through a long wavelength pass Corning 2-73 colored glass filter, opaque to light of wavelength shorter than 560 nm. Using this filter with $YbCp^*_2$ in ether allows selective irradiation of the broad charge-transfer band centered at 680 nm in the visible spectrum.

Collection and Reduction of X-ray Intensity Data. Crystals of $[Yb_5Cp^*_6(\mu_4\text{-}F)(\mu_3\text{-}F)_2(\mu\text{-}F)_6]\cdot C_6H_5CH_3$, $YbCp^*_2\cdot OEt_2$, and $YbCp^*_2F\cdot THF$ were sealed in glass capillaries under nitrogen and mounted on a Syntex P3 diffractometer. Crystal system, space group, and unit-cell dimensions of each crystal were determined at −100 °C. Intensity data was collected by using the ω-scan technique, with background measurements at both ends of the scan. The intensities of three standard reflections were monitored periodically, and only statistical fluctuations were noted.

Solution and refinement of the structures was carried out on a VAX/IBM cluster system using a local program set. The structure of $[Yb_5Cp^*_6(\mu_4\text{-}F)(\mu_3\text{-}F)_2(\mu\text{-}F)_6]\cdot C_6H_5$ was solved by MULTAN, while the heavy-atom positions for $YbCp^*_2\cdot OEt_2$ and $[Yb_5Cp^*_6(\mu_4\text{-}F)(\mu_3\text{-}F)(_2(\mu\text{-}F)_6]\cdot C_6H_5CH_3$ were obtained via Patterson analysis. Phasing of the reflections for the remaining light atoms was accomplished via the usual combination of structure factor, Fourier synthesis, and full-matrix least-squares refinement, with anisotropic thermal parameters for all non-hydrogen atoms as well as idealized hydrogen coordinates as fixed atom contributors. The atomic scattering factors were taken from the tabu-

(33) Bosbury, P. W. L.; Fields, R.; Hazeldine, R. N. *J. Chem. Soc., Perkin Trans.* **1978**, 422–427.

(34) (a) Campbell, S. F.; Hudson, A. G.; Mooney, E. F.; Pedler, A. E.; Stephens, R.; Wood, K. N. *Spectrochim. Acta* **1967**, *23A*, 2119–2125. (b) Roylance, J.; Tatlow, J. C.; Worthington, R. E. *J. Chem. Soc.* **1954**, 4426–4429. (c) Hudson, A. G.; Pedler, A. E.; Tatlow, J. C. *Tetrahedron* **1969**, *25*, 4371–4374.

(35) Evans, D. E. M.; Feast, W. J.; Stephens, R.; Tatlow, J. C. *J. Chem. Soc.* **1963**, 4828–4834.

Table II. Pertinent Bond Lengths and Bond Angles for Ytterbium Fluoride Complexes[a]

	$YbCp^*_2F\cdot OEt_2$	$YbCp^*_2F\cdot THF$	$[Yb_5Cp^*_6F_9]\cdot C_6H_5CH_3$
	Bond Lengths (Å)		
Yb(1)-F(1)	2.015 (4)	2.026 (2)	2.387 (5)
Yb(1)-F(2)			2.342 (5)
Yb(1)-F(3)			2.319 (6)
Yb(1)-F(4)			2.175 (5)
Yb(1)-F(5)			2.191 (5)
Yb(2)-F(1)			2.378 (5)
Yb(2)-F(2)			2.326 (6)
Yb(2)-F(3)			2.336 (5)
Yb(2)-F(6)			2.214 (5)
Yb(2)-F(7)			2.192 (5)
Yb(3)-F(1)			2.365 (5)
Yb(3)-F(2)			2.468 (6)
Yb(3)-F(4)			2.183 (5)
Yb(3)-F(6)			2.210 (6)
Yb(3)-F(8)			2.217 (5)
Yb(4)-F(1)			2.373 (5)
Yb(4)-F(3)			2.450 (6)
Yb(4)-F(5)			2.207 (5)
Yb(4)-F(7)			2.198 (5)
Yb(4)-F(9)			2.205 (5)
Yb(5)-F(8)			2.192 (5)
Yb(5)-F(9)			2.212 (5)
Yb(1)-O(1)	2.378 (5)	2.330 (3)	
O(1)-C(1)	1.468 (10)	1.456 (6)	
O(1)-C(2)	1.435 (12)	1.461 (5)	
C(1)-C(3)	1.474 (14)	1.485 (7)	
C(2)-C(4)	1.345 (18)	1.503 (7)	
C(3)-C(4)		1.513 (7)	
$Yb(1)-C_R(av)$[b]	2.631 (8)	2.628 (5)	2.600 (8)
$Yb(2)-C_R(av)$			2.603 (9)
$Yb(3)-C_R(av)$			2.616 (9)
$Yb(4)-C_R(av)$			2.625 (9)
$Yb(5)-C_R(av)$			2.618 (9)
Yb(1)···Yb(3)			3.4515 (7)
Yb(1)···Yb(4)			3.4483 (7)
Yb(2)···Yb(3)			3.4548 (9)
Yb(2)···Yb(4)			3.4509 (8)
	Bond Angles (deg)		
F(1)-Yb(1)-O(1)	85.0 (2)	86.3 (1)	
F(8)-Yb(5)-F(9)			88.2 (2)
F(1)-Yb(2)-F(2)			65.3 (2)
F(1)-Yb(2)-F(6)			71.0 (2)
F(1)-Yb(3)-F(2)			63.3 (2)
F(1)-Yb(3)-F(8)			72.1 (2)
F(2)-Yb(2)-F(3)			76.3 (2)
F(2)-Yb(3)-F(4)			71.5 (2)
F(2)-Yb(3)-F(8)			135.1 (2)
F(4)-Yb(3)-F(6)			137.7 (2)
F(4)-Yb(3)-F(8)			90.7 (2)
F(6)-Yb(2)-F(7)			101.2 (2)
Yb(1)-F(1)-Yb(2)			95.7 (2)
Yb(1)-F(1)-Yb(3)			93.2 (2)
Yb(1)-F(2)-Yb(2)			98.4 (2)
Yb(1)-F(2)-Yb(3)			91.7 (2)
Yb(2)-F(2)-Yb(3)			92.2 (2)
Yb(1)-F(4)-Yb(3)			104.7 (2)
Yb(3)-F(1)-Yb(4)			170.5 (2)
Yb(3)-F(8)-Yb(5)			158.6 (2)

[a] A complete set of bond distances and angles is included with the supplementary material. Selected data given here is primarily pertinent to ytterbium–fluorine bonding and is representative of chemically equivalent distances and angles in the rest of the molecule (which may vary by up to 0.02 Å and 2°). [b] $Yb-C_R(av)$ is the average Yb–C bond length for the Cp* ring carbon atoms; individual distances can be found in the supplementary material.

lations of Cromer and Waber: anomalous dispersion corrections were by Cromer.[36a] In the least-squares refinement the function minimized was $(\sum w|F_o| - |F_c|)^2$ with the weights, w, assigned as $1/\sigma^2(F_o)$. Standard deviations of observed reflections, $\sigma(F_o)$, were derived by using counting statistics and a p value of 0.02.[36b] Reflections were discarded when the condition $(F_o^2) > n\sigma(F_o^2)$ did not hold, the values of n being listed in Table I, section d, under the entry "$I = n(I)$, n".

A summary of selected crystal and refinement data is given in Table I, while Table II shows selected geometric data. Full details of the three structures including data collection and refinement parameters, the final positional and thermal parameters, general temperature factors, calculated hydrogen atom positions, structure factor listings, and a complete tabulation of bond distances and angles are available.[37]

(36) (a) *International Tables for X-ray Crystallography*; Kynoch Press: Birmingham, England, 1974; Vol. IV: (i) Table 2.2B; (ii) Table 2.3.1. (b) Corfield, P. W. R.; Doedens, R. J.; Ibers, J. A. *Inorg. Chem.* **1967**, *6*, 197–204.

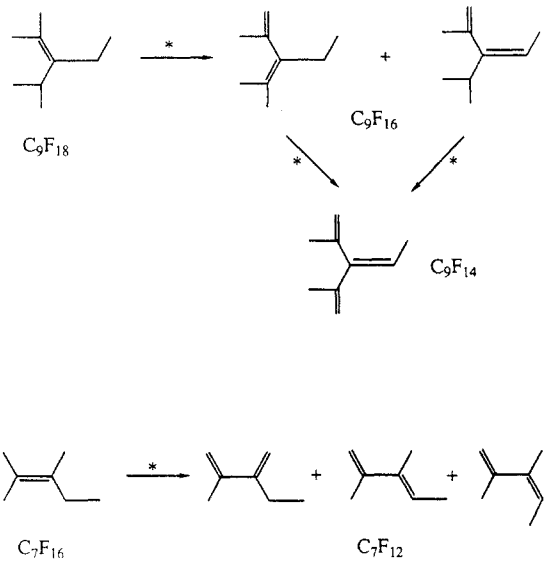

Figure 1. Conversion of perfluoro enes to perfluoro dienes and perfluoro trienes occurs readily by using divalent lanthanoid reagents (denoted by the asterisk in the figure) MCp^*_2 (M = Yb, Eu and Sm) and $YbCp'_2$ in ether, THF, or toluene at room temperature. The reactions are illustrated above for the perfluoro enes C_9F_{18} and C_7F_{14}.

Results and Discussion

Perfluoroolefin Reactivity. While some carbon–fluorine bonds are reported to be inert toward intermolecular halide atom abstraction by divalent lanthanoids,[14] we have found classes of fluoro compounds where abstraction of fluorine atoms does occur readily. These compounds include perfluoroolefins in which an allylic fluorine is removed initially from sp^3 carbon or, in cases where that is less favorable, initially from an olefinic sp^2 carbon. Also included are perfluoroarenes, where fluorine is necessarily removed from sp^2 carbon, although rates for these reactions are much lower than for the allylic fluorine abstractions. The mechanisms of these reactions are undoubtedly analogous to previously studied halogen atom abstraction reactions between divalent lanthanoids MCp^*_2 and bromo-, chloro-, or iodoalkanes.[7,15]

Each of the lanthanoid complexes $MCp^*_2\cdot OEt_2$ (M = Yb, Sm, Eu) and $YbCp'_2\cdot OEt_2$ reacts rapidly with C_9F_{18}, perfluoro-2,4-dimethyl-3-ethylpent-2-ene, or C_7F_{14}, perfluoro-2,3-dimethylpent-2-ene, in toluene or ether solutions (typically 0.05 M in each reagent) at 25 °C. Visible spectroscopy of the organometallic products and reactants (see Experimental Section) in principle provides a simple method for measuring the rates of these reactions. However at room temperature the rates are so fast that this is not possible even at submillimolar concentrations of the

(37) See paragraph at end of paper regarding supplementary material.

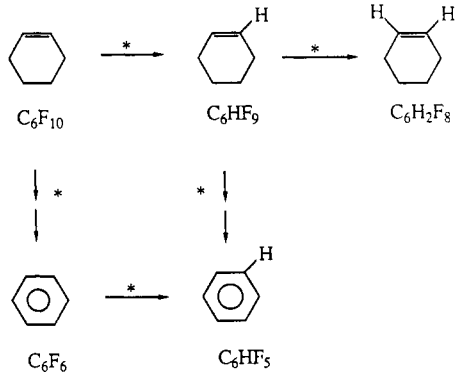

Figure 2. The four products shown above are identified from reactions of MCp^*_2 (M = Yb, Eu, Sm) and $YbCp'_2$ (denoted by the asterisk in the figure) with perfluorocyclohexene and result from two parallel radical abstraction pathways which require removal of a fluorine atom either from the olefinic position or from the allylic position of perfluorocyclohexene.

reactants. The initially formed fluoroorganic products are the isomeric C_9F_{16} perfluoro dienes and the C_9F_{14} perfluoro triene from perfluoro-2,4-dimethyl-3-ethylpent-2-ene and three isomeric C_7F_{12} perfluoro dienes from perfluoro-2,3-dimethylpent-2-ene as shown in Figure 1. The trivalent lanthanoid monofluorides MCp^*_2F (M = Yb, Sm, Eu) and $YbCp'_2F$ are the initially formed organometallic products from reaction of either the C_9F_{18} or the C_7F_{14} olefin. The reactions are virtually stoichiometric. With 2:1 ratios of metal to either C_9F_{18} or C_7F_{14} perfluoroolefin, the overall recovery of perfluorinated organics is >95%, with >90% actual yields of isomeric dienes (plus the previously unknown C_9F_{14} triene product, in the reaction of C_9F_{18}) by ^{19}F NMR.

Perfluoroolefins are less reactive, and the reactions are more complicated if abstraction of fluorine at an allylic site does not give a perfluorinated allyl radical having at least three carbon substituents. One example of this is the reaction of perfluoro cyclohexene with each of the four complexes $MCp^*_2{\cdot}OEt_2$ (M = Yb, Sm, Eu) and $YbCp'_2{\cdot}$THF, the products of which are shown in Figure 2. Fluorinated benzenes C_6F_6 and C_6F_5H are formed by multiple fluorine atom abstraction, but the primary initial product is 2,3,3,4,4,5,5,6,6-nonafluorocyclohexene, which results from abstraction of fluorine at the olefinic sp^2 carbon. Secondary organics 3,3,4,4,5,5,6,6-octafluorocyclohexene and pentafluorobenzene are also characterized as products in these reactions and derive from multiple fluorine abstraction from the first-formed nonafluorocyclohexene. Pentafluorobenzene may also form via fluorine abstraction followed by H atom addition from the other aromatic product perfluorobenzene. However, qualitative observation of the rates of reaction of perfluorobenzene directly with the divalent lanthanoids suggests that these reactions are sufficiently slow by comparison with the rates of reaction of perfluorocyclohexene that formation and subsequent reaction of perfluorobenzene is certainly not the only route for formation of pentafluorobenzene from perfluorocyclohexene. Fluorine bonded to sp^2 carbon indeed is abstracted from hexafluorobenzene by all four lanthanoid reagents but at least an order of magnitude slower in each case than the corresponding rate of reaction of perfluorocyclohexene. The reaction product is mainly pentafluorobenzene with some perfluorobiphenyl. No perfluorobiphenyl is observed in the reactions of perfluorocyclohexene which we studied here.

Deuterium-labeling studies indicate that the hydrogen source for the transformations shown in Figure 2 is not the solvent but probably the pentamethylcyclopentadienyl rings of the organometallic reagents $MCp^*_2{\cdot}OEt_2$ and $YbCp'_2{\cdot}OEt_2$. For sample, when the reactions are run in diethyl-d_{10} ether as solvent (where the coordinated ether immediately undergoes ligand exchange), only C_6HF_9 and not C_6DF_9 is observed by GC–MS and proton-coupled ^{19}F NMR. Obviously the yield of organometallic products MCp^*_2F, which is formed stoichiometrically from reactions of the C_9F_{18} and C_7F_{16} (vide supra), is lowered in these reactions of perfluorocyclohexene.

We isolated the four trivalent fluoride products $YbCp^*_2F$, $YbCp'_2F$, $SmCp^*_2F$, and $EuCp^*_2F$ as ether or THF adducts from reactions of the C_9F_{18} and C_7F_{16} with the corresponding divalent lanthanoid. The ytterbium complex $YbCp^*_2F$ was characterized by X-ray crystallography as both the ether and the THF solvates (the structures are described in detail below). The infrared absorption bands assigned to the M–F stretching modes in these fluoride complexes ($YbCp^*_2F$, 303 cm^{-1}; $YbCp'_2F$, 326 cm^{-1}; $SmCp^*_2F$, 304 cm^{-1}; $EuCp^*_2F$, 311 cm^{-1}) occur at low frequency compared to monomeric three-coordinate MF_3 compounds (high-frequency modes for EuF_3, 530, 504 cm^{-1}, and for YbF_3, 569, 546 cm^{-1}) studied by matrix isolation,[38] as expected considering that the eight-coordinate complexes would have considerably longer bond lengths. No infrared data for other organolanthanoid fluoride complexes are available for comparison.

Secondary Products. A complicating feature of the fluorine atom abstractions is the observation of secondary products, both fluoro organic and organometallic. The fluoro organic secondary product shown in Figure 1 is the highly unsaturated C_9F_{14} perfluoro triene, derived from the perfluoro dienes by further fluorine atom removal. The organometallic secondary products result from Cp* for F exchange, i.e., the formation of trivalent MCp^*F_2 species from the first-formed trivalent MCp^*_2F complexes. A cluster that we isolated from the ytterbium system $YbCp^*_2$ and characterized by X-ray crystallography has the stoichiometry $[Yb_5Cp^*_6(\mu_4\text{-}F)(\mu_3\text{-}F)_2(\mu\text{-}F)_6]$. The structure of this complex, isolated as a toluene solvate, is described fully below.

Recently Andersen[8,39] published the structures of two extremely interesting mixed-valent ytterbium complexes with bridging fluorides of overall stoichiometry $[YbCp^*_2F]_2[YbCp^*F]_2$ and $Yb_2Cp^*_4F$, each containing both Yb(II) and Yb(III) atoms. Isolation of the first material from reaction of $YbCp^*_2$ with AgF,[39] and the second material from the reaction of unsolvated $YbCp^*_2$ with perfluorobenzene[8] (and other reagents), complements our isolation of a larger, completely trivalent cluster with stoichiometry $[Yb_5Cp^*_6(\mu_4\text{-}F)(\mu_3\text{-}F)_2(\mu\text{-}F)_6]$. To emphasize the components, $[Yb_5Cp^*_6(\mu_4\text{-}F)(\mu_3\text{-}F)_2(\mu\text{-}F)_6]$ could also be written as $[YbCp^*_2F(YbCp^*F_2)_4]$.

These materials suggest that two pathways can exist for the formation of $YbCp^*F_2$ from $YbCp^*_2$, i.e., through either $YbCp^*F$ or $YbCp^*_2F$ as intermediates. Put another way, fluoride for Cp* exchange can occur either before or after oxidation from divalent to trivalent state. We consider the possibility unlikely that Andersen's clusters or our cluster are isolated because of a particular thermodynamic stability. A more likely scenario is that a ratio of $YbCp^*_2$, $YbCp^*F$, $YbCp^*_2F$, $YbCp^*F_2$, and even potentially YbF_3 in the product mixture is formed as a function of the amount of oxidizing fluorine reagent in the system and its

(38) Hauge, R. H.; Hastie, J. W.; Margrave, J. L. *J. Less Common Met.* **1971**, *23*, 359–365.
(39) Burns, C. J.; Berg, D. J.; Andersen, R. A. *J. Chem. Soc., Chem. Commun.* **1987**, 272–273.

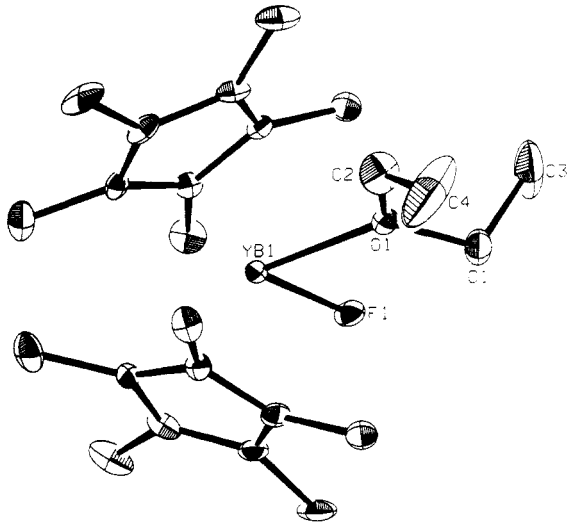

Figure 3. A side-view ORTEP drawing shows the molecular structure, determined by X-ray crystallography, of complex $YbCp^*_2F{\cdot}OEt_2$ which contains a terminal fluoride ligand a coordinated diethyl ether ligand.

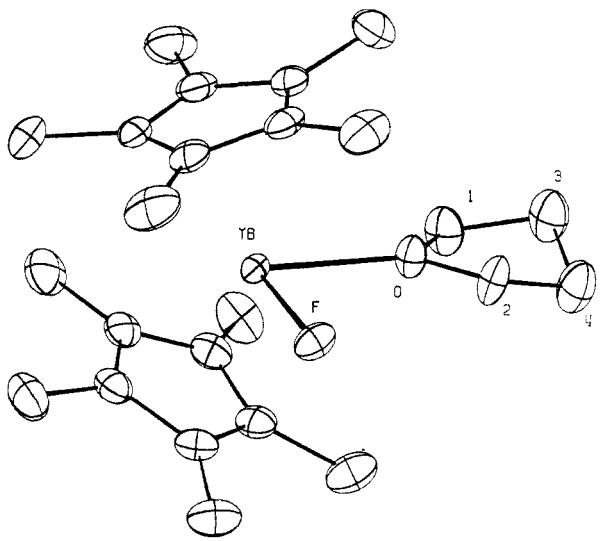

Figure 4. The THF-solvated complex $YbCp^*_2F{\cdot}THF$ also contains a terminal fluoride ligand, illustrated in this shaded ORTEP drawing.

relative rates of reaction with the varous organometallic species. The cluster that crystallizes presumably tends to reflect this ratio and maximize the number of bridging fluorine bonds. The implication is that the clusters mentioned here are only two of a potential family of related cluster complexes. Andersen's clusters need not be viewed as intermediates in the oxidation of $YbCp^*_2$ to $[Yb_5Cp^*_6(\mu_4\text{-}F)(\mu_3\text{-}F)_2(\mu\text{-}F)_6]$, but the constituent fragments such as $YbCp^*_2F$ and $YbCp^*F$ probably are. Undoubtedly fluoride clusters can also be formed with the larger ions Sm and Eu in di- or trivalent or mixed-valent oxidation states when the metal ions have only one Cp* (or are otherwise rather sterically unencumbered), but we did not attempt to synthesize such molecules.

Structural Details from X-ray Crystallography. Tables I and II list pertinent crystal, data reduction, and geometric data for the X-ray crystallographic study of $YbCp^*_2F{\cdot}OEt_2$, $YbCp^*_2F{\cdot}OEt_2$, $YbCp^*_2F{\cdot}THF$, and $[Yb_5Cp^*_6(\mu_4\text{-}F)(\mu_3\text{-}F)_2(\mu\text{-}F)_6]$. Complete details of the structures are provided in the supplementary material, which is available as noted at the end of this paper. ORTEP representations of the three molecules are shown in Figures 3, 4, and 5.

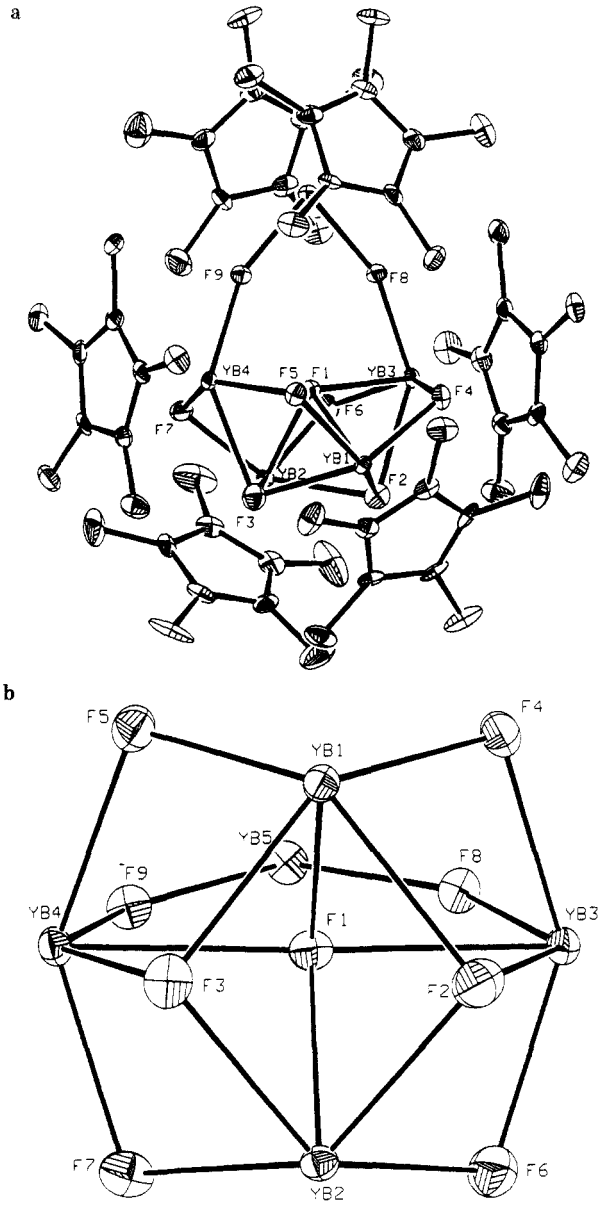

Figure 5. (a) An ORTEP representation of the structure of the trivalent ytterbium fluoride cluster $[Yb_5Cp^*_6(\mu_4\text{-}F)(\mu_3\text{-}F)_2(\mu\text{-}F)_6]$ shows that all fluorine atoms in this molecule are in bridging positions. (b) An expanded view of the Yb_5F_9 core of the cluster $[Yb_5Cp^*_6(\mu_4\text{-}F)(\mu_3\text{-}F)_2(\mu\text{-}F)_6]$ gives a clearer view of the different bridging fluoride environments.

No terminal lanthanoid–fluorine bond distances have been reported in the literature to date. The values found here for $YbCp^*_2F{\cdot}OEt_2$ and $YbCp^*_2F{\cdot}THF$, 2.015 and 2.026 Å, are close to the value of 2.082 Å which would be expected by subtracting the difference, 0.45 Å, in Pauling's crystal radii[40] of chloride (1.81 Å) and fluoride (1.36 Å) ions from a terminal ytterbium–chloride bond distance, for example, in the structure of $YbCp^*_2Cl{\cdot}(Me_2PCH_2PMe_2)$,[41] 2.532 Å. No significant differences were found between the $YbCp^*_2F$ cores in the crystal structures of the ether and THF adducts of $YbCp^*_2F$. Ytterbium–fluorine, –oxygen, and –carbon bonds are all similar in the two compounds. The structures of $YbCp^*_2F{\cdot}OEt_2$ and $YbCp^*_2F{\cdot}THF$ conform to the general formula $MCp^*_2X{\cdot}Y$ (where X is a halide ion, Y = X^- or THF, and M is a

(40) Pauling, L. *The Nature of the Chemical Bond*, 3rd ed.; Cornell University Press: Ithaca, NY, 1973; p 514.
(41) Tilley, T. D.; Andersen, R. A.; Zalkin, A. *Inorg. Chem.* **1983**, *22*, 856–859.

lanthanoid and group III metal), a number of which have now been crystallographically studied.[42] Comparison of the MCp^*_2 bonding of the structures reported here with those in the literature reveals nothing exceptional. The novelty of $YbCp^*_2F{\cdot}OEt_2$ and $YbCp^*_2F{\cdot}THF$ lies in the characterization of terminal ytterbium–fluorine bonds and the diethyl ether ligand. The structure of the diethyl ether complex is included to illustrate the conformation of the diethyl ether ligand when coordinated to a metal, since such examples are not common in the literature. The diethyl ether carbon–carbon bonds in $YbCp^*_2F{\cdot}OEt_2$ are transoid with respect to the ytterbium–oxygen bond and oriented to minimize steric interactions within the coordination environment. The conformation is similar to the lithium-bound diethyl ether ligands in $YbCp^*_2X_2Li(OEt_2)_2$ (X = Cl, I), previously characterized by X-ray crystallography.[42b]

The geometry of the $[Yb_5Cp^*_6(\mu_4\text{-}F)(\mu_3\text{-}F)_2(\mu\text{-}F)_6]$ fluoride-bridged cluster is essentially a capped butterfly arrangement of ytterbium atoms, each of which is eight-coordinate when the Cp* ligands are counted as three-coordinate (see Figure 5). The cap is a $YbCp^*_2$ unit while the vertices of the butterfly are YbCp* units. All ytterbium atoms are trivalent. The capping ytterbium is in a pseudotetrahedral environment, and two of the ligands are bridging fluorines. The four remaining ytterbiums (symmetrically there are two sets of two) are each coordinated to five bridging fluorine atoms. As seen from Figure 5, all of the fluorine atoms in the molecule occupy bridging sites and all are fairly symmetrical (in the sense of being essentially equidistant from the ytterbiums to which they are coordinated). The molecule contains four chemically distinct sets of bridging fluorine atoms: two sets of fluorines bridge two ytterbium atoms (referred to as "doubly bridging"), one set bridges three ytterbium atoms (referred to as "triply bridging"), and a fourth unique fluorine atom is coordinated to all four ytterbium atoms in the butterfly part of the cluster. The average bond length of the doubly bridging fluorine atoms which join the $YbCp^*_2$ unit with two of the YbCp* units is 2.206 (5) Å, very close to the average bond length of 2.196 (5) Å for the doubly bridging fluorine atoms within the butterfly unit. Comparison with the terminal Yb–F distances in the $YbCp^*_2F{\cdot}OEt_2$ and $YbCp^*_2F{\cdot}THF$ structures shows that bridging between two ytterbiums causes an average bond lengthening of about 0.16 Å. Bond lengths for the bridging fluorines do not seem to be affected by the angle of bend at fluorine, since the Yb–F–Yb bond angle for the former set is 158.6° while this angle for the latter set averages only 103.6°.

The triply bridging fluorines of cluster $[Yb_5Cp^*_6(\mu_4\text{-}F)(\mu_3\text{-}F)_2(\mu\text{-}F)_6]$ are slightly further (average 2.459 Å) from one ytterbium than from the other two (average 2.331 Å), with the overall average bond length of 2.374 Å. The three Yb–F–Yb angles for these two fluorines average 98.6, 92.15, and 92.25° (see Table II for F(2) data). The unique fluorine is in an unusual environment because the four ytterbiums to which it is bonded are situated as if at the vertices of an octahedron having two adjacent vertices missing. These four Yb–F bonds are similar in length, averaging 2.375 Å, indistinguishable from the averaged Yb–F bond length of a triply bridging fluorine.

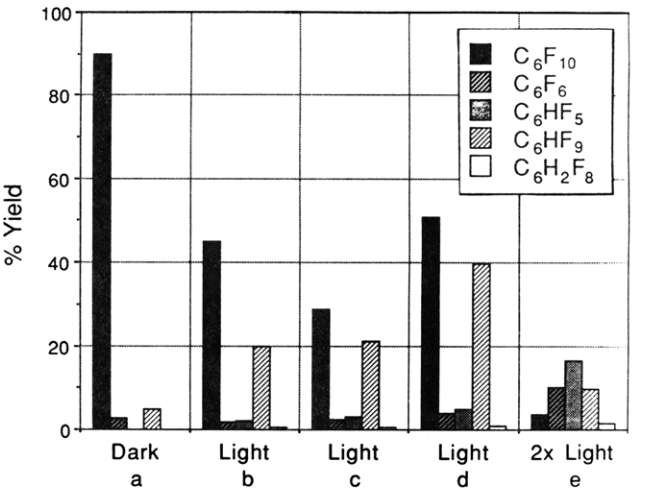

Figure 6. Quantitative product distributions for reaction of ytterbium complex $YbCp^*_2{\cdot}OEt_2$ with perfluorocyclohexene in a mixture of ether (0.6 mL) and C_6D_6 (0.2 mL) at 26 °C for 30 min are given for the conditions: (a) Yb complex (0.2 mmol), C_6F_{10} (0.05 mmol); (b) Yb complex (0.1 mmol), C_6F_{10} (0.1 mmol), with <560-nm light filter as described in the Experimental Section; (c) Yb complex (0.1 mmol), C_6F_{10} (0.1 mmol); (d) Yb complex (0.2 mmol), C_6F_{10} (0.05 mmol), (e) Yb complex (0.2 mmol), C_6F_{10} (0.05 mmol). Irradiation conditions "light" and "2× light" are described in the Experimental Section. These data show that visible light of wavelength greater than 560 nm causes more rapid defluorination of perfluorocyclohexene by $YbCp^*_2OEt_2$ than does the thermal reaction alone.

Comparison of the Yb–F bond lengths of doubly bridging fluorine sets of $[Yb_5Cp^*_6(\mu_4\text{-}F)(\mu_3\text{-}F)_2(\mu\text{-}F)_6]$ (2.196 (5) and 2.206 (5) Å) with the doubly bridging fluorines in Andersen's tetranuclear complex $[YbCp^*_2F]_2[YbCp^*F]_2$ (2.129 (2) and 2.220 (2) Å) shows little difference. This is somewhat surprising, since the latter complex is mixed-valent and might be expected to exhibit longer bond length due to the larger ionic radius of divalent ytterbium. The bond lengths of 2.317 (2) and 2.084 (2) Å in the asymmetric molecule $Yb_2Cp^*_4F$ (viewed by Andersen as a donor–acceptor complex) span the ranges of bond lengths observed for the apparently more electronically delocalized larger clusters just mentioned. There are few other examples to use for comparison; however, our values for Yb–F bond lengths compare well with orthorhombic crystals of YbF_3.[43] Here the ytterbium is eight-coordinate and the sum of the ionic radii of Yb^{3+} (0.970 Å) and F^- (1.295 Å) is found to be 2.265 Å. A complex of the smaller trivalent ion scandium $Sc(C_5H_5)_2F$ is the only structurally analogous group III complex in the literature, and it exists as a trimer with bridging fluorines.[44] The difference between our bond distances for doubly bridging Yb–F (average 2.201 (2) Å) and similar Sc–F bonds in the trimer (average 2.046 (8) Å) is reasonable considering the difference (0.12 (1) Å) in Shannon's ionic radii[45] for the two metals.

Light-Enhanced Fluorine Abstraction. During studies of the abstraction of fluorine from perfluorocyclohexene using $YbCp^*_2{\cdot}OEt_2$, it became apparent that

(42) (a) Baker, E. C.; Brown, L. D.; Raymond, K. N. *Inorg. Chem.* **1975**, *14*, 1376–1379. (b) Watson, P. L.; Whitney, J. F.; Harlow, R. L. *Inorg. Chem.* **1981**, *20*, 3271–3278. (c) Tilley, T. D.; Andersen, R. A. *Inorg. Chem.* **1981**, *20*, 3267–3270. (d) Tilley, T. D.; Andersen, R. A. *J. Am. Chem. Soc.* **1982**, *104*, 1772–1774. (e) Boncella, J. M.; Andersen, R. A. *Inorg. Chem.* **1984**, *23*, 432–437. (f) Evans, W. J.; Grate, J. W.; Levan, K. R.; Bloom, I.; Peterson, T. T.; Doedens, R. J.; Zhang, H.; Atwood, J. L. *Inorg. Chem.* **1986**, *25*, 3614–3619. (g) Gong, L.; Streitwieser, A.; Zalkin, A. *J. Chem. Soc., Chem. Commun.* **1987**, 460–461. (h) Evans, W. J.; Drummond, D. K.; Grate, J. W.; Zhang, H.; Atwood, J. L. *J. Am. Chem. Soc.* **1987**, *109*, 3928–3936. (i) Deacon, G. B.; Fallon, G. D.; MacKinnon, P. I.; Newnham, R. H.; Pain, G. N.; Tuong, T. D.; Wilkinson, D. L. *J. Organomet. Chem.* **1984**, *277*, C21–C24. (j) Albrecht, I.; Haan, E.; Pickardt, J.; Schumann, H. *Inorg. Chim. Acta* **1985**, *110*, 145–147.

(43) Greis, O.; Petzel, T. *Z. Anorg. Allg. Chem.* **1973**, *403*, 1–22.

(44) Bottomley, F.; Paez, D. E.; White, P. S. *J. Organomet. Chem.* **1985**, *291*, 35–41.

(45) Shannon, R. D. *Acta Crystallogr.* **1976**, *A32*, 751–767.

light enhances both the rate and the yield of the reaction. The products from this reaction (pentafluorobenzene, 2,3,3,4,4,5,5,6,6-nonafluorocyclohexene, 3,3,4,4,5,5,6,6-octafluorocyclohexene, and perfluorobenzene) form in 25–40% recovered yield over several hours at 25 °C. However, exposure to visible light (as indicated in the Experimental Section) causes the same reaction in a half hour. In fact, we observed that the defluorination reaction was promoted by visible light for all of the lanthanoid reagents studied. Even $EuCp^*_2$, which showed no reaction with C_6F_{10} in the dark within 30 min, gave 10% conversion to C_6HF_9 when the reaction mixture (in a Pyrex tube) was exposed to light from a tungsten lamp for 30 min ($EuCp^*_2$, 0.25 M, and C_6F_{10}, 0.065 M). Examples of reaction products obtained under various conditions (dark, light, and filtered) are illustrated in Figure 6 for reagent $YbCp^*_2$ (in Figure 6; the term "light" refers to the tungsten lamp setup described in the Experimental Section, "2× light" means that the lamp was moved to a position 6 in. from the sample). The yield of C_6HF_9 and secondary products such as $C_6H_2F_8$ increase with light relative to the yield observed in the dark reaction. Visible light filtered to pass only wavelengths greater than 560 nm also causes the same increase in yield, e.g. experiment b in Figure 6. This indicates that the broad absorption band centered at 680 nm in the visible spectrum of $YbCp^*_2$ is responsible for the photochemistry. While the quantum yields for these reactions are not known, the effect of light in promoting the reaction is none-the-less clear. Undoubtedly the excited-state metal complex has an enhanced reduction potential[46] and a sufficiently long lifetime to encounter with substrate in solution and thereby can increase the observed rate of defluorination.

Ellis measured the absorption and photoluminescence spectra[47] of $YbCp^*_2$·THF and MCp^*_2·OEt_2 (M = Yb, Eu),[48] establishing the excited state lifetime of $EuCp^*_2$·OEt_2 to be 400 ± 40 ns. Such long lifetimes are typical for lanthanide ions and are well documented.[49] Chemiluminescence from $YbCp^*_2$·OEt_2 during a decomposition reaction with oxygen was also reported.[50] These results, together with our qualitative observations on light promotion of the defluorination reactions discussed above, suggest that such fluorine abstractions may be genuine excited-state photochemical reactions, having well-defined products in this case. It should be noted that light-promoted reactions of fluorocarbons alone, including fluorine-transfer reactions in the absence of metals, have been reported in the literature.[11] However, these require high-energy irradiation in the UV range and hence are not responsible for the chemistry described here.

Reduction Potentials. Ytterbium, europium, and samarium in the +2 oxidation state are quite reducing metal ions, with reduction potentials in the region between −0.5 and −2.5 V (depending on metal, ligand, and solvent), decreasing in the order Sm > Yb > Eu. In particular, samarium (usually as the diiodide) has been used widely as a one-electron reducing agent for organic carbonyl compounds, but a variety of uses of divalent lanthanoids in organic synthesis have been reviewed.[51-54] Since the fluorine atom abstraction reactions are formally metal oxidation reactions, the ease of such reactions would be expected to parallel increasingly negative reduction potentials. Although the reactions of perfluoro-2,3-dimethylpent-2-ene with MCp^*_2·OEt_2 (M = Yb, Sm, Eu) are too fast to measure kinetics by standard visible spectroscopy, the qualitative observation can be made that rates are in the order Sm > Yb > Eu (at millimolar dilutions in ether the Sm reaction is virtually instantaneous while the Eu reaction takes several minutes). Qualitatively the same trend holds true for reaction of perfluorocyclohexene, where the absolute rates are much slower than for perfluoro-2,3-dimethylpent-2-ene. In fact the Eu compound is unreactive at room temperature within 30 min while the Sm compound reacts instantly. The trend is again true for perfluorobenzene, where the absolute rates of fluorine atom abstraction in ether are much slower even than for perfluorocyclohexene. Perfluorobenzene reacts with $YbCp^*_2$·OEt_2 (both 0.1 M in ether) negligibly at 25 °C in the dark. When the temperature is raised to 50 °C, about 10% of the perfluorobenzene is converted to mainly pentafluorobenzene over a period of 3 h with the same reagents. As expected from the reduction potentials, reaction between hexafluorobenzene and $SmCp^*_2$·OEt_2 is much faster (over in 15 min at 25 °C) whereas the same reaction with $EuCp^*_2$·OEt_2 is much slower (no observed reaction over 48 h).

We measured the M(III)/M(II) reduction potentials of acetonitrile-solvated complexes MCp^*_2 (M = Yb, Sm, Eu) and $YbCp'_2$ in acetonitrile by cyclic voltammetry. The values (referenced internally to ferrocene and quoted relative to ferrocene[30]) are as follows: $EuCp^*_2$, −1.22 V; $YbCp'_2$, −1.65 V; $YbCp^*_2$, −1.78 V; $SmCp^*_2$, −2.41 V. The values are 0.8–0.9 V more negative than for the corresponding lanthanoid perchlorate 2+/3+ couple in acetonitrile.[55,56] Although the absolute potentials in diethyl ether solution would be different than in acetonitrile (since the solvent actually coordinates to the metal), the relative potentials are not expected to change dramatically (e.g., see electrochemical studies of lanthanoid complexes of crown ethers in a variety of solvents[57,58]).

While it is evident that reduction potential of the metal is usually the dominant contributor to reactivity, steric factors could also be important in inner-sphere atom abstraction because perfluorocarbons are often inherently sterically congested molecules (note that the covalent radius of fluorine is almost twice that of hydrogen[59]). From X-ray crystal structures of complexes MCp^*_2·OEt_2 (M = Yb, Sm, Eu) and $YbCp'_2$ (as the glyme adduct)[28] the coordination cones available for substrate coordination in the

(46) Bock, C. R.; Connor, J. A.; Gutierrez, A. R.; Meyer, T. J.; Whitten, D. G.; Sullivan, B. P.; Nagle, J. K. *J. Am. Chem. Soc.* **1979**, *101*, 4815–4824.
(47) Thomas, A. C.; Ellis, A. B. *È* **1984**, *31* and *32*, 564–566.
(48) Thomas, A. C.; Ellis, A. B. *Organometallics* **1985**, *4*, 2223–2225.
(49) Edelstein, N. M., Ed. *Lanthanide and Actinide Chemistry and Spectroscopy*; American Chemical Society: Washington, DC, 1980. For examples: Chapter 14, M. J. Weber, pp 275–311; Chapter 17, J. P. Hessler, and W. T. Carnall, pp 349–368.
(50) Thomas, A. C.; Ellis, A. B. *J. Chem. Soc., Chem. Commun* **1984**, 1270–1271.
(51) Namy, J. L.; Girard, P.; Kagan, H. B. *Nouv. J. Chim.* **1981**, *5*, 479–484.
(52) (a) Namy, J. L.; Collin, J.; Zhang, J.; Kagan, H. B. *J. Organomet. Chem.* **1987**, *328*, 81–86. (b) Namy, J. L.; Girard, P.; Kagan, H. B. *Nouv. J. Chim.* **1977**, *1*, 5–7. (c) Kagan, H. B.; Namy, J. L.; Girard, P. *Tetrahedron* **1981**, *37*, W175. (d) Namy, J. L.; Souppe, J.; Collin, J.; Kagan, H. B. *J. Org. Chem.* **1984**, *49*, 2045–2049.
(53) (a) Molander, G. A.; Etter, J. B. *Tetrahedron Lett.* **1984**, *25*, 3281–3284. (b) Gemal, A. L.; Luche, J. L. *J. Am. Chem. Soc.* **1981**, *103*, 5454–5459 and references therein.
(54) Kagan, H. B.; Namy, J. L. *Handbook on the Physics and Chemistry of the Rare Earths*; Gschneidner, K. A., Eyring, L., Eds.; (Elsevier Science Publishers B. V.), 1984; pp 525–565.
(55) Mikheev, N. B. *Inorg. Chim. Acta* **1984**, *94*, 241–248.
(56) Cokal, E. J.; Wise, E. N. *J. Electroanal. Chem.* **1966**, *12*, 136–147, 170–171.
(57) Tabib, J.; Hupp, J. T.; Weaver, M. J. *Inorg. Chem.* **1986**, *25*, 1916–1918.
(58) Massaux, J.; Desreux, J. F.; Delchambre, C.; Duyckaerts, G. *Inorg. Chem.* **1980**, *19*, 1893–1986.
(59) Pauling, L. *The Nature of the Chemical Bond*, 3rd ed.; Cornell University Press: Ithaca, NY, 1973; pp 165, 168.

solvent free MCp'_2[26,27] moieties are approximately: M = Yb, 125°; M = Sm, 128°; M = Eu, 128°; and $YbCp'_2$, 170° (expressed as the largest C–M–C′ angle where the carbons are methyls attached to opposite C_5 rings and oriented toward the "open" coordination site). While arguments can be made regarding mobility of the rings to accommodate incoming ligands and relative surface areas presented by the metals at the open site due to varying ionic radii (Yb, 1.22 Å, Eu, 1.34 Å, Sm, 1.36 Å, for seven-coordinate divalent ions),[45] none-the-less the degree of steric hindrance at the metal is clearly much less for $YbCp'_2$ than for any of the Cp* derivatives.

Of the Cp* complexes, the ytterbium reagent is marginally less hindered than the samarium or europium derivatives. An example of *selectivity* due to sterics is seen with the relative rates of formation of the two C_9F_{16} dienes shown in Figure 1. The ratio of perfluoro-2-methyl-3-isopropylpenta-1,3-diene to perfluoro-2,4-dimethyl-3-ethylpenta-1,3-diene at low conversion reflects their relative rates of formation, which varies with the lanthanoid reagent: $YbCp^*_2$ (5.2) > $EuCp^*_2$ (2.9) > $YbCp'_2 \approx SmCp^*_2$ (1). The selectivities (but not necessarily the absolute rates) thus correlate with size effects rather than reduction potential.

Conclusions

In an apparently general reaction, divalent lanthanoid complexes MCp^*_2 (M = Yb, Sm, Eu) and $YbCp'_2$ rapidly defluorinate certain perfluoroolefins, e.g., perfluoro-2,3-dimethylpent-2-ene, via sequential fluorine atom abstraction reactions from the allylic positions of the perfluoroolefin and intermediate perfluoroallyl radicals. This provides a convenient synthesis of the resulting organometallic trivalent monofluorides MCp^*_2F (M = Yb, Sm, Eu) and $YbCp'_2F$ which are isolated in crystalline form as ether or THF solvates. The photolytic promotion of these fluorine atom abstraction reactions by visible light deserves further investigation, since many potential fluoro organic substrates reach much more slowly than the examples studied here.

Reactions of $YbCp^*_2{\cdot}OEt_2$ an $EuCp^*_2{\cdot}OEt_2$ with perfluoro-2,3-dimethylpent-2-ene are noticeably faster in toluene than in ether, consistent with ether loss from the coordination sphere followed by inner-sphere fluorine atom abstraction.[7,15] This suggests the existence of transient intermediates, $MCp^*_2{\cdot}F{-}R_f$, where lone pairs on the fluorine atoms of the perfluorocarbons acts as weak Lewis bases, coordinating to Lewis acidic divalent MCp^*_2 species. Andersen's $Yb_2Cp^*_4F$ dimer provides an example of such a donor–acceptor interaction, although the fluorine atom in this case is a very good donor due to the highly polarized fluorine–ytterbium bond. Existence of such fluorine donor interaction with the less polarized fluorine–ytterbium bond. Existence of such fluorine donor interaction with the less polarized fluorine–carbon bond is supported by San Filippo's report of the use of trivalent lanthanoid complexes (also weak Lewis acids) as NMR chemical shift reagents for alkyl fluorides.[60] In transition-metal chemistry, the phenomenon of covalent alkyl halides acting as Lewis bases has been verified crystallographically by Crabtree, including the intramolecular chelation of fluorine (in 8-fluoroquinoline) to iridium.[61] Although π-donor olefin and acetylene complexes of lanthanoids have recently been described by Wayda[62] and Andersen,[63] it is unlikely that the tetrasubstituted, electron-deficient π-bonds of the perfluoroolefins used here would form transient intermediates of this type. Instead, the fluorine atoms of such olefins are the more likely site of complexation by a Lewis acid.

The structures of $YbCp^*_2F{\cdot}OEt_2$ and $YbCp^*_2F{\cdot}THF$ derived from X-ray crystallography provide the first lanthanoid–fluorine terminal bond distances, 2.015 and 2.026 Å, respectively. Much slower secondary reaction of the perfluoroolefins with the lanthanoid trivalent monofluorides gives trivalent difluorides. For example, $YbCp^*_2F$ is slowly converted to $YbCp^*F_2$ which is one of the "building blocks" of the isolated pentaytterbium cluster $[Yb_5Cp^*_6(\mu_4\text{-}F)(\mu_3\text{-}F)_2(\mu\text{-}F)_6]$. However, the intimate mechanism of Cp*-for-F exchange in the reaction remains unknown.

Acknowledgment. Discussions with B. Smart, W. Farnham, and F. Weigert were most helpful and are gratefully acknowledged. Excellent technical assistance of L. C. Petrovich is much appreciated.

Registry No. $YbBr_2{\cdot}THF_2$, 113173-30-1; $YbI_2{\cdot}THF_2$, 120368-70-9; $EuI_2{\cdot}THF_2$, 123882-26-8; $SmI_2{\cdot}THF_2$, 94138-28-0; $YbCp^*_2{\cdot}OEt_2$, 74282-47-6; $EuCp^*_2{\cdot}OEt_2$, 84254-55-7; $SmCp^*_2{\cdot}OEt_2$, 85962-90-9; $YbCp'_2$, 104764-82-1; $YbCp'_2{\cdot}THF$, 76137-73-0; $YbCp^*_2F{\cdot}THF$, 123882-27-9; $EuCp^*_2F{\cdot}OEt_2$, 123902-66-9; $SmCp^*_2F{\cdot}OEt_2$, 123882-28-0; $YbCp'_2F{\cdot}THF$, 123882-29-1; $[Yb_5Cp^*_6(\mu_4\text{-}F)(\mu^3\text{-}F)_2(\mu\text{-}F)_6]{\cdot}C_6H_5CH_3$, 123882-31-5; $YbCp^*_2F{\cdot}OEt_2$, 117470-41-4; KCp*, 94348-92-2; KCp', 41066-45-9; Yb, 7440-64-4; Eu, 7440-53-1; Sm, 7440-19-9; C_7F_{14}, 58621-65-1; C_9F_{18}, 30320-26-4; C_9F_{14}, 123902-65-8; C_6F_{10}, 355-75-9; C_6HF_9, 777-97-9; $C_6H_2F_8$, 775-40-6; C_6HF_5, 363-72-4; C_6F_6, 392-56-3; $C_{12}F_{10}$, 434-90-2; perfluoro-2,4-dimethyl-3-ethylpenta-1,3-diene, 79743-71-8; perfluoro-2-methyl-3-ethylbuta-1,3-diene, 123882-24-6; perfluoro-(*E*)-2,3-dimethylpenta-1,3-diene, 67544-94-9; perfluoro-(*Z*)-2,3-dimethylpenta-1,3-diene, 67544-92-7; perfluoro-2-methyl-3-isopropylpenta-1,3-diene, 123882-25-7; dibromoethane, 25620-62-6; diiodoethane, 31627-74-4.

Supplementary Material Available: Full details of the crystal structures discussed in the text including listings of crystal data, fractional coordinates and isotropic thermal parameters, anisotropic thermal parameters, and bond distances and angles and a drawing for $YbCp^*_2F{\cdot}OEt_2$, crystal data, ORTEP drawings, and bond distances and angles for Yb-$Cp^*_2F{\cdot}THF$, crystal data, fractional coordinates and isotropic thermal parameters, anisotropic thermal parameters, bond distances and angles, fixed hydrogen atom positions, and ORTEP drawings for $Yb_5Cp^*_6F_9{\cdot}C_6H_5CH_3$, and positional parameters, refined temperature factor expressions, and general temperature factor expressions for $YbCp^*_2F_9{\cdot}C_6H_5CH_3$ (39 pages); listings of structure factors for $YbCp^*_2F{\cdot}OEt_2$, $YbCp^*_2F_9{\cdot}C_6H_5CH_3$, and $Yb_5Cp^*_6F_9{\cdot}C_6H_5CH_3$ (45 pages). Ordering information is given on any current masthead page.

(60) San Filippo, J., Jr.; Nuzzo, R. G.; Romano, L. J. *J. Am. Chem. Soc.* **1975**, *97*, 2546.

(61) Kulawiec, R. J.; Holt, E. M.; Lavin, M.; Crabtree, R. H. *Inorg. Chem.* **1987**, *26*, 2559–2561.

(62) Andrews, M. P.; Wayda, A. L. *Organometallics* **1988**, *7*, 743–9.

(63) (a) Burns, C. J.; Andersen, R. A. *J. Am. Chem. Soc.* **1987**, *109*, 915–917. (b) Burns, C. J.; Andersen, R. A. *J. Am. Chem. Soc.* **1987**, *109*, 941–942.